Numerical simulation of heat source properties of pulsed tungsten inert gas arc†

ITO Kuniyoshi*, TASHIRO Shinichi* and TANAKA Manabu*

KEY WORDS: (Numerical simulation) (Pulsed TIG arc) (Heat source property)

1. Introduction

The heat source properties of TIG arc strongly depend on the composition of shielding gas. For example, since the arc column is constricted due to low electrical conductivity of the helium arc, heat flux onto a base metal in case of helium TIG arc is higher than that of argon TIG arc. The heat source properties can be controlled also by current waveform. Pulsed TIG welding is suitable for back-bead welding and thin plate welding, because the heat flux onto the base metal can be controlled by adjusting peak / base current ratio and frequency. A number of results on experimental and theoretical investigations of the heat source properties of DC TIG arc have been reported. However, those of pulsed TIG arc are still not fully understood because of the complexity of the phenomenon. In this study, the heat source properties of pulsed TIG arc for various shielding gas composition were numerically analyzed.

2. Simulation Model

The calculation region for TIG arc consists of a tungsten cathode with diameter of 3.2mm and tip angle of 60 degrees, arc plasma and a water-cooled copper anode. It is described in a frame of cylindrical coordinate with axial symmetry around the arc axis. The electrode gap is set to be 5mm. Argon (Ar), helium (He) or carbon dioxide (CO_2) is introduced as shielding gas from the upper boundary at the flow rate of 10 l min^{-1}. For example of physical properties of each gas, specific heat, thermal conductivity and electrical conductivity are shown in **Fig. 1**. **Figure 2** shows current wave form with the peak current of 150A and the base current of 50A. The frequency is 100Hz and the pulse width is 5ms. The laminar flow is assumed, and the arc plasma is considered to be in the local thermodynamic equilibrium (LTE). The governing equations (1)-(6) are solved iteratively by the SIMPLEC numerical procedure [1]. The other numerical modeling methods are given in detail in our previous paper [2].

(1) Mass continuity equation

$$\frac{\partial \rho}{\partial t}+\frac{1}{r}\frac{\partial}{\partial r}(r\rho v_r)+\frac{\partial}{\partial r}(\rho v_z)=0$$

(2) Radial momentum conservation equation

$$\frac{\partial \rho v_r}{\partial t}+\frac{1}{r}\frac{\partial}{\partial r}(r\rho v_r^2)+\frac{\partial}{\partial z}(\rho v_z v_r)=-\frac{\partial P}{\partial r}-j_z B_\theta + \frac{1}{r}\frac{\partial}{\partial r}(2r\eta\frac{\partial v_r}{\partial r})+\frac{\partial}{\partial z}(\eta\frac{\partial v_r}{\partial z}+\eta\frac{\partial v_z}{\partial r})-2\eta\frac{v_r}{r^2}$$

(3) Axial momentum conservation equation

$$\frac{\partial \rho v_z}{\partial t}+\frac{1}{r}\frac{\partial}{\partial r}(r\rho v_r v_z)+\frac{\partial}{\partial z}(\rho v_z^2)=-\frac{\partial P}{\partial z}+j_r B_\theta + \frac{\partial}{\partial z}(2\eta\frac{\partial v_z}{\partial z})+\frac{1}{r}\frac{\partial}{\partial r}(r\eta\frac{\partial v_r}{\partial z}+r\eta\frac{\partial v_z}{\partial r})+\rho g$$

(4) Energy conservation equation

$$\frac{\partial \rho h}{\partial t}+\frac{1}{r}\frac{\partial}{\partial r}(r\rho v_r h)+\frac{\partial}{\partial z}(\rho v_z h)=\frac{1}{r}\frac{\partial}{\partial r}(\frac{r\kappa}{c_p}\frac{\partial h}{\partial r})+\frac{\partial}{\partial z}(\frac{\kappa}{c_p}\frac{\partial h}{\partial z}) + j_r E_r + j_z E_z - U$$

(5) Current continuity equation

$$\frac{1}{r}\frac{\partial}{\partial r}(rj_r)+\frac{\partial}{\partial z}(j_z)=0$$

(6) Ohm's law

$$j_r=-\sigma E_r,\ j_z=-\sigma E_z$$

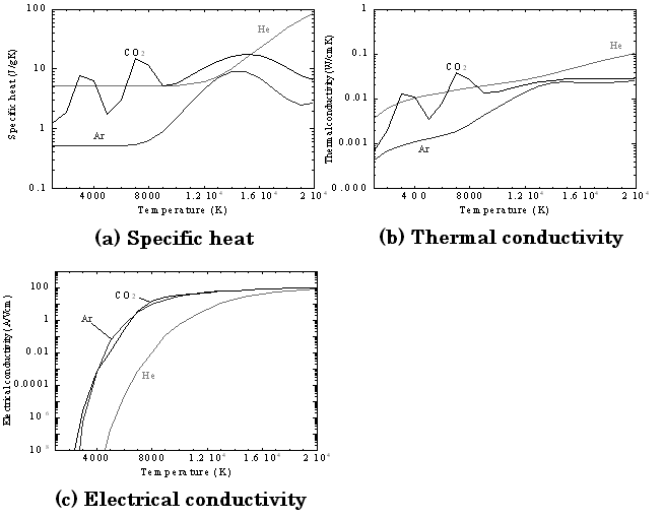

(a) Specific heat (b) Thermal conductivity

(c) Electrical conductivity

Fig. 1 Physical properties of shielding gas

† Received on 30 September 2010
* JWRI, Osaka University, Osaka, Japan

Transactions of JWRI is published by Joining and Welding Research Institute, Osaka University, Ibaraki, Osaka 567-0047, Japan

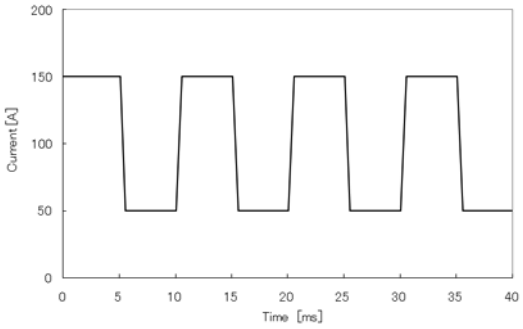

Fig. 2 Current wave form

In the above equations, t is time, h is enthalpy, P is pressure, v_z and v_r are the axial and radial velocities, j_z and j_r are the axial and radial component of current density, g is acceleration due to gravity, κ is thermal conductivity, C_p is specific heat, ρ is density, η □□ is viscosity, σ is electrical conductivity, U is radiation emission coefficient, E_r and E_z are the radial and axial components of the electric field defined by $E_r = -\partial V/\partial r$ and $E_z = -\partial V/\partial z$, where V is electric potential.

3. Results and Discussion

Figure 3 shows two-dimensional temperature distributions at t=30ms,32.5ms,35ms and 37.5ms in the case of Ar. During the peak current, the heat caused by Joule heating near the cathode tip was transported toward the anode by convective flow and was also transported in a radial direction by thermal conduction. **Figure 4** shows two-dimensional temperature distributions in the case of CO_2. In this case, although the heat transport toward the anode by convective flow was seen, that in the radial direction due to thermal conduction was smaller than that of Ar because of influence of large specific heat. As a result, the radius of the arc column hardly changed during the calculation. Finally **Fig. 5** shows two-dimensional temperature distributions in the case of He. It was seen that the temperature distribution changed momentarily following the change in the arc current due to high thermal conductivity of He.

4. Conclusions

(1) In the case of Ar, the heat caused by Joule heating near the cathode tip was transported toward the anode by convective flow and was also transported in a radial direction by thermal conduction.
(2) In CO_2, although the heat transport toward the anode by convective flow was seen, that in the radial direction due to thermal conduction was smaller than that of Ar because of influence of large specific heat.
(3) In the case of He, the temperature distribution changed momentarily following the change in the arc current due to high thermal conductivity of He.

References

[1] S.V. Patanker: Numerical heat transfer and fluid flow, Hemishpere Publishing Corporation (1980).

[2] M. Tanaka, et.al.: Plasma Chem. Plasma Process, 23 (2003), 585-606.

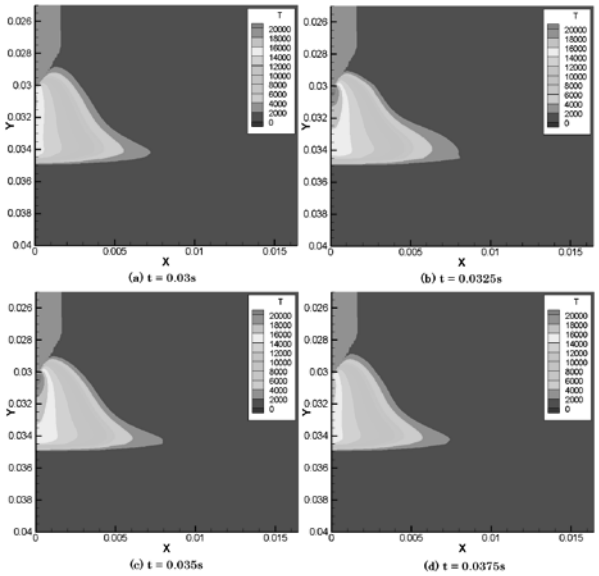

Fig. 3 Temperature distribution (Ar)

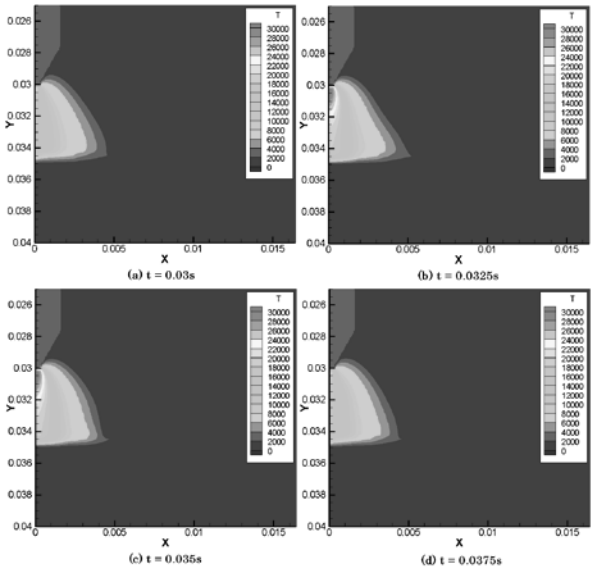

Fig. 4 Temperature distribution (CO_2)

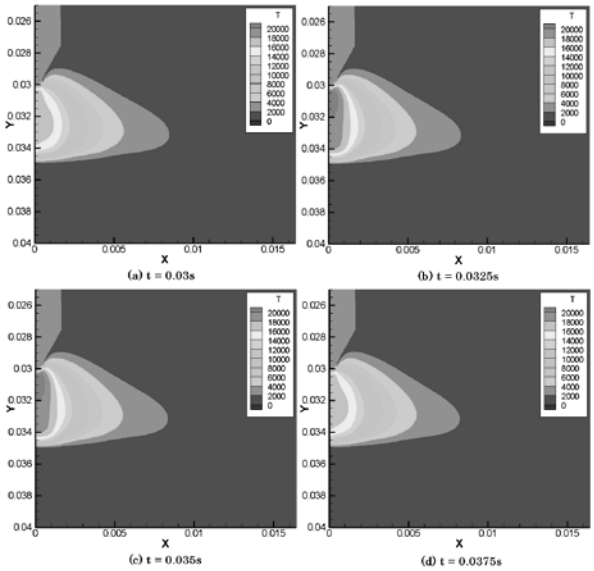

Fig. 5 Temperature distribution (He)